

Passivation effects on ZnO nanowire field effect transistors under oxygen, ambient, and vacuum environments

Sunghoon Song, Woong-Ki Hong, Soon-Shin Kwon, and Takhee Lee^{a)}

Department of Materials Science and Engineering, Gwangju Institute of Science and Technology, Gwangju 500-712, Republic of Korea

(Received 16 January 2008; accepted 14 June 2008; published online 2 July 2008)

We investigated the passivation effects on the electrical characteristics of ZnO nanowire field effect transistors (FETs) under the various oxygen environments of ambient air, dry O₂, and vacuum. When the ZnO nanowire FET was exposed to more oxygen, the current decreased and the threshold voltage shifted to the positive gate bias direction, due to electrons trapping to the oxygen molecules at the nanowire surface. On the contrary, the electrical properties of the nanowire FET remained unchanged under different environments with passivation by a polymethyl methacrylate layer, which demonstrates the importance of surface passivation for ZnO nanowire-based electronic device applications. © 2008 American Institute of Physics. [DOI: 10.1063/1.2955512]

One-dimensional nanostructures have potential as building blocks for nanoelectronic device applications and are currently the subject of intensive research. Because of this, single-crystalline nanostructures of semiconducting metal oxides such as ZnO, In₂O₃, and SnO₂ have been extensively studied.^{1–3} Among these, ZnO nanowires are important materials for nanoscale devices, such as ultraviolet lasers, light-emitting diodes, photodetectors, chemical sensors, and solar cells, due to their direct wide bandgap (3.37 eV) semiconducting properties, and large exciton binding energy (60 meV).^{4–8} In the mean time, semiconductor surfaces are strongly affected by the chemical adsorption of ambient gases.^{9,10} Similarly, the electrical properties of semiconducting nanowires, including ZnO nanowires, are significantly influenced by chemisorption of ambient gases, primarily oxygen.^{11–13} Particularly, the partial pressure of oxygen has a significant influence on the electrical performance of ZnO nanowire field effect transistors (FETs). This is due to the change of conductivity caused by surface energy band bending, induced by O₂ molecule adsorption.¹⁴ The oxygen molecules adsorbed at the defect sites of ZnO nanowires, such as oxygen vacancies, act as electron acceptors and form oxygen ions (O⁻, O²⁻, or O₂⁻).^{15,16} Then, these chemisorbed oxygen ions deplete the surface electrons and reduce the channel conductivity.¹⁴ For this reason, surface passivation has been employed to prevent oxygen molecules from being adsorbed onto the nanowire. For example, Chang *et al.* reported that a SiO₂/Si₃N₄ passivation improved the device performance of ZnO nanowire FETs.¹⁷

In this letter, we report on a detailed study of the passivation effects on the ZnO nanowire FETs under different oxygen environments of ambient air, dry O₂, and a vacuum. The FET devices were fabricated with ZnO nanowires grown on a ZnO film coated sapphire substrate, and were passivated with a polymethyl methacrylate (PMMA) layer. The electrical properties of the ZnO nanowire FETs were investigated and compared before and after the PMMA passivation under different environments.

The ZnO nanowires used in this study were grown by a vapor transport method on a ZnO film-coated sapphire sub-

strate. The details of the growth method have been explained elsewhere.¹⁸ The grown ZnO nanowires were characterized using high resolution transmission electron microscopy (HRTEM). Then, in order to fabricate the ZnO nanowire FET devices, ZnO nanowires were first transferred from the growth substrate to a silicon wafer with a 100-nm-thick thermally grown oxide, by dropping a nanowire suspension in ethanol on the silicon wafer. The silicon wafer is a highly doped *p*-type silicon, which can be used as a back gate electrode. Additionally, metal electrodes consisting of Ti (100 nm)/Au (100 nm) were deposited by an electron beam evaporator and defined as source and drain electrodes, by photolithography and a lift-off process. The distance between the source and drain electrodes was typically 3–4 μm. Then, we measured the electrical characteristics of the ZnO nanowire FET devices under ambient air, dry O₂, and vacuum environments. After measurement, we performed a surface passivation process on the nanowire FETs using PMMA to prevent the effect of O₂ adsorption during air exposure. After the passivation process, the nanowire FET devices were subsequently characterized at the same environments; ambient air, dry O₂, and vacuum. The transistor characteristics of the ZnO nanowire FETs were measured using a semiconductor parameter analyzer (HP4145B).

Figure 1(a) shows the typical HRTEM image of a ZnO nanowire grown on a ZnO film coated sapphire substrate. The inset of Fig. 1(a) is the fast Fourier transform pattern of

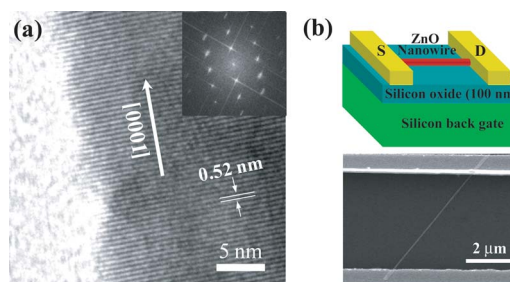


FIG. 1. (Color online) (a) HRTEM image of the ZnO nanowires grown on a ZnO film coated sapphire substrate. Inset is the fast Fourier transform pattern. (b) Schematic of a ZnO nanowire FET device structure (top) and FESEM image of a single ZnO nanowire connected between source and drain electrodes in a FET device (bottom).

^{a)}Electronic mail: tlee@gist.ac.kr.

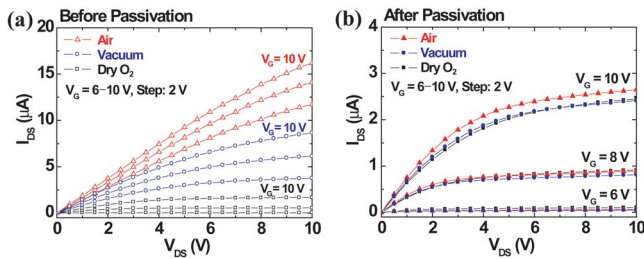


FIG. 2. (Color online) Output characteristics (I_{DS} - V_{DS}) for different gate biases (from 6 to 10 V, with a step of 2 V) for the ZnO nanowire FET, acquired under ambient air, dry O_2 , and vacuum conditions (a) before and (b) after passivation.

the ZnO nanowire. These results indicate that the ZnO nanowire is single crystal with a preferred growth direction of [0001]. Figure 1(b) shows a schematic of a ZnO nanowire FET device structure (top) and the field emission scanning electron microscopy image of a single ZnO nanowire connected between the source and drain electrodes in a FET device (bottom).

Figure 2 shows a series of the source-drain current versus voltage (I_{DS} - V_{DS}) curves measured at different gate voltages (from 6 to 10 V with a step of 2 V) under various environments of ambient air (20% O_2), dry O_2 , and vacuum ($\sim 10^{-3}$ Torr). Figures 2(a) and 2(b) display the I_{DS} - V_{DS} characteristics for a ZnO nanowire FET before and after passivation, respectively. As shown in Fig. 2(a), the current level was significantly affected by the environmental condition with O_2 molecules. The currents decreased significantly when the ZnO nanowire FET was exposed to dry O_2 , as compared to the case in ambient air. When the oxygen was evacuated, the currents increased again. These phenomena can be explained by oxygen effects. As mentioned previously, the ambient oxygen partial pressure has a considerable effect on the electrical properties of ZnO nanowire FETs.¹⁴ Particularly, the adsorbed oxygen molecules deplete the electrons in the ZnO nanowire and form oxygen ions (O^- , O^{2-} , or O_2^-).¹⁶ Then, the electrons in the ZnO nanowires are trapped by the adsorbed oxygen molecules, and thus the surface depletion region of ZnO nanowire can be formed, leading to current reduction and threshold voltage shift to the positive gate bias direction [Fig. 3(a)]. As the oxygen pressure is raised, more electrons are captured by the oxygen molecules at the nanowire surface. As a result, the depletion region is widened and the carrier density in the ZnO nanowire is decreased even more. On the contrary, the I_{DS} - V_{DS} curves in Fig. 2(b) indicate that after passivation there is a negligible effect on the ZnO nanowire FET by oxygen mol-

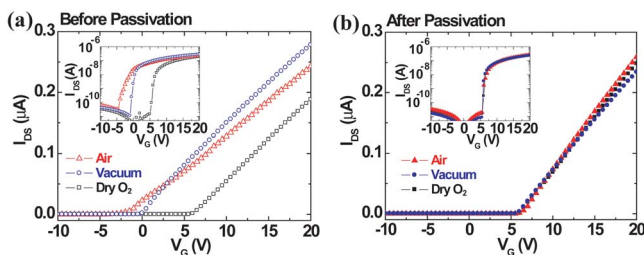


FIG. 3. (Color online) Transfer characteristics (I_{DS} - V_G) at $V_{DS}=0.1$ V for the ZnO nanowire FET, acquired under ambient air, dry O_2 , and vacuum conditions (a) before and (b) after passivation. The insets show the semi-logarithmic plot of the I_{DS} - V_G curves.

ecules in different oxygen environments. This is because the PMMA passivation layer prevents oxygen molecules from being adsorbed onto the nanowire. One can also notice that the ZnO nanowire FETs after passivation have a better electrical performance in terms of well-defined linear and saturation regions in I_{DS} - V_{DS} curves [Fig. 2(b)]. It has been reported that the passivation can improve the FET performance by enhancing the gate coupling effect.^{19,20}

This passivation effect is more prominent in transfer characteristics (I_{DS} - V_G curves), as summarized in Fig. 3. A series of plots in Fig. 3 show the I_{DS} - V_G curves measured at a fixed source-drain voltage, $V_{DS}=0.1$ V under the same different environments of ambient air (20% O_2), dry O_2 , and vacuum ($\sim 10^{-3}$ Torr). Figures 3(a) and 3(b) present the I_{DS} - V_G curves for the ZnO nanowire FET before and after passivation, respectively. The I_{DS} - V_G plots in the semilogarithmic scale (insets of Fig. 3) show an on/off current ratio as large as 10^4 - 10^5 for both before and after passivation.

The threshold voltage is defined as the gate voltage obtained by extrapolating the linear portion of the I_{DS} - V_G curve from the point of maximum slope to zero drain current, in which the point of maximum slope is the point where transconductance (dI_{DS}/dV_G) is at a maximum.²¹ Before passivation [Fig. 3(a)], the threshold voltages of ZnO nanowire FET shifted from -1.73 V (in ambient air) to 6.05 V (in dry O_2) in the positive gate bias direction. This is because more electrons are captured by the oxygen as the oxygen pressure is raised. As a result, the depletion layer is widened and the carrier density in the ZnO nanowire is decreased when the FET is exposed to dry O_2 environment. Since the charge density is reduced after being exposed to dry O_2 , more positive gate bias is needed to make currents flow in the nanowire channel, thus the threshold voltage shifts to the positive gate bias direction. When oxygen gas was evacuated to a vacuum level of 10^{-3} Torr, the threshold voltages of the nanowire FET shifted back from 6.05 V (in dry O_2) to -0.10 V (in a vacuum) in the negative gate bias direction. This is due to reduction of the trapping effects of oxygen in a vacuum. On the contrary, when the FET was passivated with PMMA, the threshold voltages were ~ 6 V and shifted very little under different oxygen environments, as shown in Fig. 3(b). Although the threshold voltages of the passivated ZnO nanowire FET look similar to that of unpassivated nanowire in dry O_2 (Fig. 3), the carrier concentration, mobility, subthreshold swing [$SS=d(V_G)/d(\log I_{DS})$] values are different (Fig. 4). For example, we obtained the SS values of ~ 1570 , ~ 490 , and ~ 440 mV/decade for the unpassivated ZnO nanowire FET measured in ambient air, dry O_2 , and in vacuum, respectively. After the passivation, the SS improved as it decreased to ~ 380 mV/decade for all the three cases of different environments, which is due to the enhancement of gate coupling effect by embedment of nanowire between the gate oxide and the passivation layer. Note that although the ambient air is intermediate between dry O_2 and vacuum in terms of oxygen concentration, we have not observed that the transistor parameters of the ZnO nanowire FET follow the oxygen concentration. For example, the mobility and SS swing was the worst for the unpassivated nanowire FET measured in ambient air among the three different environmental cases [Fig. 4(b)]. Other factors such as nanowire morphology, dimension, and interfacial effect between nanowire and insulating layers would also affect the nanowire devices.

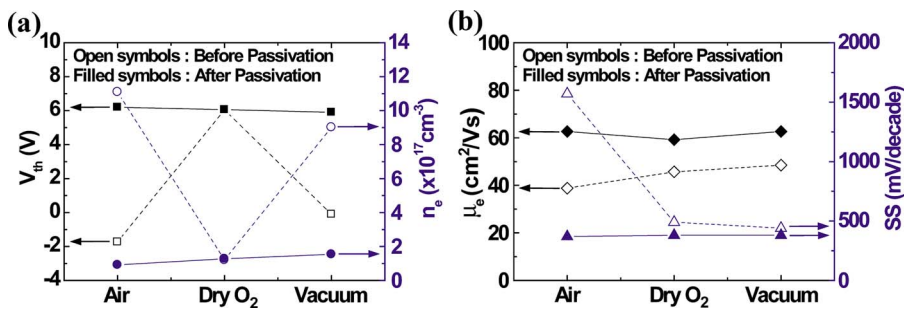


FIG. 4. (Color online) (a) Threshold voltage (V_{th}) and carrier concentration (n_e), (b) mobility (μ_e) and SS for the ZnO nanowire FET under ambient air, dry O₂, and vacuum conditions before and after passivation.

Recently, we have observed the surface roughness of ZnO nanowire can significantly influence its electronic transport properties.²²

The threshold voltages can be used to estimate the carrier concentration from the total charge, $Q_{tot} = C_g |V_G - V_{th}|$ in the nanowire, where C_g is the gate capacitance and V_{th} is the threshold voltage required to deplete the nanowire.¹⁸ The gate capacitance C_g can be estimated using a model of a cylinder on an infinite metal plate,^{18,23}

$$\frac{C_g}{L} = \frac{2\pi\epsilon\epsilon_0}{\cosh^{-1}\left(\frac{r+h}{r}\right)}, \quad (1)$$

where r is the nanowire radius (~ 42.5 nm), L is the nanowire channel length (~ 4 μ m), h is the SiO₂ thickness (100 nm), ϵ_0 is the permittivity of free space, and ϵ is the dielectric constant of SiO₂ (3.9). Thus, the carrier concentration, $n_e = Q_{tot}/e\pi r^2 L$, can be determined at a gate bias of 7 V for the ZnO nanowire FET in ambient air, dry O₂, and vacuum before and after passivation, as summarized in Fig. 4(a). Here, 7 V was arbitrarily chosen because the ZnO nanowire is on-current state for all the cases at this voltage (Fig. 3). Before passivation, the carrier concentration in the ZnO nanowire was estimated as $\sim 1.1 \times 10^{18}$ cm⁻³ in ambient air, and was then decreased to $\sim 1.2 \times 10^{17}$ cm⁻³, when the FET is exposed to the dry O₂ environment. This is because more electrons are captured by the oxygen molecules in the dry O₂ environment. Then, when oxygen gas was evacuated to a vacuum level of $\sim 10^{-3}$ Torr, the carrier concentration was increased to $\sim 9.0 \times 10^{17}$ cm⁻³. After passivation, the carrier concentration is nearly 1.6×10^{17} cm⁻³, regardless of the different oxygen environments. The carrier mobility (μ_e) and the SS values of the ZnO nanowire FET are also plotted in Fig. 4(b). The carrier mobility in the low field region can be calculated by

$$\mu_e = \frac{dI_{DS}}{dV_G} \frac{L^2}{V_{DS} C_g}. \quad (2)$$

Through this calculation, we obtained μ_e of ~ 39 cm²/V s (air), 46 cm²/V s (dry O₂), and 49 cm²/V s (vacuum) before passivation and ~ 60 cm²/V s regardless of the different oxygen environments after passivation, indicating that the carrier mobility of ZnO nanowire FET was slightly improved after passivation.

In summary, we have fabricated FET devices using ZnO nanowires, grown by the vapor transport method on a ZnO film-coated sapphire substrate, and have characterized their electrical properties under the various oxygen environments, before and after passivation by the PMMA. With more oxygen environments, the unpassivated ZnO nanowires FETs

were significantly influenced in terms of carrier concentration, carrier mobility, and threshold voltage. However, passivation protects ZnO nanowire FETs from oxygen exposure and maintains their electrical characteristics under different environments. This study facilitates recognizing the importance of surface passivation or protection of ZnO nanowire based electronic devices or other materials and devices.

This work was supported through the Proton Accelerator User Program by the Ministry of Science and Technology of Korea, the National Research Laboratory (NRL) Program of the Korea Science and Engineering Foundation (KOSEF), and the Program for Integrated Molecular System at GIST.

¹Z. L. Wang, *J. Phys.: Condens. Matter* **16**, R829 (2004).

²B. Lei, C. Li, D. Zhang, Q. F. Zhang, K. K. Shung, and C. Zhou, *Appl. Phys. Lett.* **84**, 4553 (2004).

³S. V. Kalinin, J. Shin, S. Jesse, D. Geohegan, A. P. Baddorf, Y. Lilach, M. Moskovits, and A. Kolmakov, *J. Appl. Phys.* **98**, 044503 (2005).

⁴P. Yang, H. Yan, S. Mao, R. Russo, J. Johnson, R. Saykally, N. Morris, J. Pham, R. He, and H.-J. Choi, *Adv. Funct. Mater.* **12**, 323 (2002).

⁵C. H. Liu, J. A. Zapfen, Y. Yao, X. M. Meng, C. S. Lee, S. S. Fan, Y. Lifshitz, and S. T. Lee, *Adv. Mater. (Weinheim, Ger.)* **15**, 838 (2003).

⁶H. Kind, H. Yan, B. Messer, M. Law, and P. Yang, *Adv. Mater. (Weinheim, Ger.)* **14**, 158 (2002).

⁷Q. Wan, Q. H. Li, Y. J. Chen, T. H. Wang, X. L. He, J. P. Li, and C. L. Lin, *Appl. Phys. Lett.* **84**, 3654 (2004).

⁸J. B. Baxter and E. S. Aydil, *Appl. Phys. Lett.* **86**, 053114 (2004).

⁹W. Mönch, *J. Vac. Sci. Technol. B* **4**, 1085 (1986), **7**, 1216 (1989).

¹⁰T. Wolkstein, in *Electronic Processes on Semiconductor Surfaces During Chemisorption*, edited by R. Morrison (Consultants Bureau, New York, 1991), p. 1991.

¹¹J. Lagowski, E. S. Sproles, Jr., and H. C. Gatos, *J. Appl. Phys.* **48**, 3566 (1977).

¹²M. Liu and H. K. Kim, *Appl. Phys. Lett.* **84**, 173 (2004).

¹³W. I. Park, J. S. Kim, G.-C. Yi, M. H. Bae, and H.-J. Lee, *Appl. Phys. Lett.* **85**, 5052 (2004).

¹⁴Z. Fan, D. Wang, P.-C. Chang, W.-Y. Tseng, and J. G. Lu, *Appl. Phys. Lett.* **85**, 5923 (2004).

¹⁵Y. Zhang, A. Kolmakov, S. Chretien, H. Metiu, and M. Moskovits, *Nano Lett.* **4**, 403 (2004).

¹⁶Q. H. Li, Y. X. Liang, Q. Wan, and T. H. Wang, *Appl. Phys. Lett.* **85**, 6389 (2004).

¹⁷P.-C. Chang, Z. Fan, C.-J. Chien, D. Stichtenoth, C. Ronning, and J. G. Lu, *Appl. Phys. Lett.* **89**, 133113 (2006).

¹⁸W. Wang, H. D. Xiong, M. D. Edelstein, D. Gundlach, J. S. Suehle, C. A. Richter, W.-K. Hong, and T. Lee, *J. Appl. Phys.* **101**, 044313 (2007).

¹⁹W.-K. Hong, D.-K. Hwang, I.-K. Park, G. Jo, S. Song, S.-J. Park, T. Lee, B.-J. Kim, and E. A. Stach, *Appl. Phys. Lett.* **90**, 243103 (2007).

²⁰O. Wunnicke, *Appl. Phys. Lett.* **89**, 083102 (2006).

²¹N. Arora, *MOSFET Models for VLSI Circuit Simulation* (Springer, Wien, New York, 1993), pp. 438–443.

²²W.-K. Hong, J. I. Sohn, D.-K. Hwang, S.-S. Kwon, G. Jo, S. Song, S.-M. Kim, H.-J. Ko, S.-J. Park, M. E. Welland, and T. Lee, *Nano Lett.* **8**, 950 (2008).

²³S. Ramo, J. R. Whinnery, and Th. Van Duzer, *Fields and Waves in Communication Electronics*, 3rd ed. (Wiley, New York, 1993).